

Time dependence of the laser-induced femtosecond lattice instability of Si and GaAs: Role of longitudinal optical distortions

P. Stampfli* and K. H. Bennemann

Theoretical Physics, Freie Universität Berlin, Arnimallee 14, D-14195 Berlin, Germany

(Received 7 September 1993)

We extend our previous analysis of the ultrafast laser-induced instability of the diamond structure of semiconductors by including longitudinal optical-phonon distortions in addition to the instability of the transverse acoustic phonons. Generally, longitudinal optical distortions enhance the instability of the transverse acoustic phonons, increasing the kinetic energy of the atoms and the final lattice temperature. These phonons make a transition to a centrosymmetric structure of GaAs with metallic properties possible. We present results for the time dependence of the instability of Si for the case where 15% of the valence electrons have been excited into the conduction band. Thus, already 100 fsec after the excitation of the plasma the atoms are displaced about 1 Å from their equilibrium position and their kinetic energy has increased to approximately 0.4 eV. Collisions between the atoms then lead to a rapid melting of the crystal. These results are in good agreement with recent experiments performed on Si and GaAs.

I. INTRODUCTION

In our previous work¹⁻³ we have shown that a very dense electron-hole plasma results in an instability of the transverse acoustic phonons of the diamond structure of Si and related semiconductors (GaAs). This is in good agreement with a series of experiments,⁴⁻¹⁰ which showed that the diamond structure of Si and GaAs becomes disordered and melts within a few hundred femtoseconds after excitation of a dense electron-hole plasma by a strong pump laser pulse. The observed threshold in the laser intensity⁹ is also obtained in our theory.

The main cause for the instability of the transverse acoustic phonons¹ is a repulsive interaction between the atoms, which arises in the presence of the electron-hole plasma. Thus we expect that longitudinal optical-phonon-like distortions should be included in our theory because they result in an additional increase in the average distance between the atoms (see Fig. 1). Actually, a recent experiment performed by Govorkov *et al.*^{5,6} on GaAs supports strongly this idea. They used a short pump laser pulse to excite a dense electron-hole plasma and a second probe laser to observe the resulting changes in the atomic structure. Time-resolved measurements of the second-harmonic generation and of the linear reflection at both the basic frequency ω and at the second harmonic 2ω have been made. From the linear reflection they obtained the corresponding time-dependent linear susceptibilities $\chi_1(\omega) \equiv [\varepsilon(\omega) - 1]/4\pi$ and $\chi_1(2\omega)$. Thus they could estimate the laser-induced time-dependent changes in the second-order susceptibility χ_2 from the observed changes in the generated second-harmonic signal. At sufficiently high pump laser intensities the second-harmonic signal vanished within 200 fsec in the experiment,⁶ which could not be explained by the time-dependent changes of the linear susceptibilities $\chi_1(\omega)$ and $\chi_1(2\omega)$ alone. In fact, they had to assume that $\chi_2(2\omega; \omega, \omega)$ vanished within less than 200 fsec after the

pump laser pulse in order to obtain a good agreement with their measurements. Note that χ_2 depends very sensitively on the atomic structure and its symmetry. Using the dipole approximation one has $\chi_2 = 0$ for the bulk of centrosymmetric materials because of the odd parity of the electric field. The diamond structure of Si has an inversion symmetry with its center in the middle of a tetrahedral bond. This symmetry is destroyed in the zinc-blende structure of GaAs because of the different valence of Ga and As. Thus GaAs is not centrosymmetric and $\chi_2 \neq 0$ before the onset of the laser pulse. On

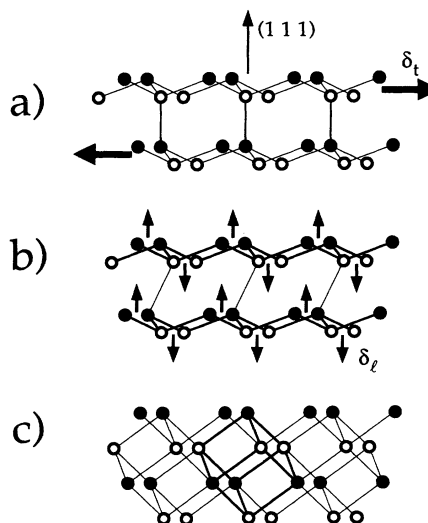


FIG. 1. Illustration of the atomic structure: (a) The ideal diamond structure, where the arrows show the transverse acoustic distortion δ_t . (b) An intermediate structure resulting from the transverse acoustic distortion. Here the arrows show the longitudinal optical distortion δ_l . (c) A new structure resulting from the combination of both distortions, which contains fragments of a simple cubic structure (shown in thick lines).

the other hand, according to the experiment⁶ χ_2 vanished within 200 fsec after the excitation of the electron-hole plasma, which implies that GaAs has become centrosymmetric. This can be achieved if the crystalline structure of GaAs makes a transformation to a new centrosymmetric configuration. Presumably, the atomic sites are then the centers of the new inversion symmetry, which requires that the distances between neighboring atomic planes (see Fig. 1) all become equal. Note that this is in strong contrast to the zinc-blende structure, where the distances between planes have a ratio of 1:3 because of tetrahedral bonding [Fig. 1(a)]. Thus a transition to a centrosymmetric structure has to involve longitudinal optical phonons at the Γ point, which change the relative distances between these planes [Figs. 1(b) and 1(c)]. This reasoning strongly suggests considering longitudinal optical phonons in a theory of the laser-induced instability of the atomic structure of Si and GaAs. Further, one expects that the gap between the valence band and the conduction band vanishes for the new highly coordinated centrosymmetric structure, resulting in metallic properties in good agreement with recent time-resolved experiments.⁷ These experiments also rule out the possibility that GaAs merely becomes amorphous (thus $\chi_2 \equiv 0$) without losing its tetrahedral bonding structure, because this would still give a nonvanishing gap and semiconducting properties.

Note that a phenomenological bond-charge model^{11,12} has been used earlier by other authors¹³⁻¹⁵ to estimate the effect of an electron-hole plasma on the equilibrium melting temperature of Si. However, the bond-charge model does not include the repulsive force due to a laser-induced electron-hole plasma. Thus one would not obtain longitudinal optical distortions from such a theory and the instability of the transverse acoustic phonon would be underestimated. From this we conclude that we need an electronic theory to examine the ultrafast laser-induced instability of the diamond or zinc-blende structure of semiconductors.

In the present paper we discuss in detail the role of the longitudinal optical-phonon distortions for the laser-induced instability of the diamond structure. Anharmonic interactions with the transverse acoustic phonons strongly enhance the effective instability of the diamond structure in comparison to previous work³ that did not include the longitudinal optical phonon. We point out that the present model is closely related to well-known mechanical properties of the diamond structure. At high hydrostatic pressure the diamond structure becomes unstable with respect to the β -tin structure. This phase transition is essentially a shear distortion of the crystal (being equivalent to a transverse acoustic phonon with wave vector $\mathbf{k}=0$), which suggests that the laser-induced electron-hole plasma similarly induces an instability of transverse acoustic phonons. Further, shear distortions related to the c_{44} shear constant involve additional atomic displacements, as first discussed by Kleinman.¹⁶ These displacements actually correspond to the longitudinal optical-phonon distortions, which are considered here. In Sec. II we present the extension of our previous theory and a detailed discussion of the physical nature of the in-

stability. Results are given in Sec. III and Sec. IV gives a short summary.

II. THEORY

First, we analyze the distortions caused by phonons and then we examine the effect of the electron-hole plasma on the cohesive energy. Finally, we discuss the effect of the plasma on the phonon frequencies and the dynamics of the instability.

A. Phonon distortions of the diamond lattice

As discussed previously¹⁻³ the diamond structure becomes unstable against shear distortions in the presence of a sufficiently dense electron-hole plasma. The resulting time-dependent average displacement of the atoms is well approximated by considering a single zone boundary phonon,³ which represents the most rapid shear distortions. Thus we obtain the dynamics of the instability from the phonon at the L point. Note that this phonon is easier to treat than other phonons because the atomic displacements can be directly obtained from the symmetries of the crystal structure (see Fig. 1).

The wave vector at the L point is $\mathbf{k}_L = \pi a_0^{-1}(1, 1, 1)/3$, where a_0 is the lattice constant of the fcc unit cell of the diamond structure. The scalar product $s = \mathbf{k}_L \mathbf{R}_0$ determines the displacement of the atom from its equilibrium position $\mathbf{R}_0 = (R_{x0}, R_{y0}, R_{z0})$. Choosing an appropriate origin it is either $s = n\pi$ or $s = (n + 1/4)\pi$, where n is an integer. Accordingly, the displacement of an atom due to this transverse acoustic phonon is either $\Delta \mathbf{R} = +\delta_l \mathbf{e}_l$ for even n or $\Delta \mathbf{R} = -\delta_l \mathbf{e}_l$ for odd n . Here δ_l is the amplitude of the phonon. We use $\mathbf{e}_l = 6^{-(1/2)}(1, 1, -2)$ as the transverse polarization vector instead of the other polarization $\tilde{\mathbf{e}}_l = 2^{-(1/2)}(1, -1, 0)$ because it results in larger average distances between the atoms. In addition we now also consider the longitudinal optical phonon at the Γ point (see Fig. 1), which has an important anharmonic interaction with the transverse acoustic phonon in the presence of the electron-hole plasma. Note the similarity to the harmonic coupling between shear distortions and the longitudinal optical phonon. This coupling causes Kleinman's internal displacement,^{16,17} which becomes important in calculations of the c_{44} elastic shear constant. However, because of the different symmetry, there is only an anharmonic interaction between the transverse acoustic phonon and the longitudinal optical phonon. The atomic displacements due to the longitudinal optical phonons are also easily determined from the symmetry of the crystal structure. They are $\Delta \mathbf{R} = -\delta_l \mathbf{e}_l$ for $s = n\pi$ and $\Delta \mathbf{R} = +\delta_l \mathbf{e}_l$ for $s = (n + 1/4)\pi$, where $\mathbf{e}_l = 3^{-(1/2)}(1, 1, 1)$ is the longitudinal polarization vector. A positive amplitude δ_l then increases the distance between those atomic planes of constant s , which are close to each other (see Fig. 1, $\Delta s = 1\pi/4$), and decreases the distance between atomic planes, which are separated by a larger distance ($\Delta s = 3\pi/4$). Note that $\delta_l = 3^{1/2}a_0/24$ results in equal distances between adjacent planes. The combination with transverse acoustic phonons then describes a transition from the diamond structure to a new sixfold coordinated

structure, which contains fragments of the simple cubic structure [Fig. 1(c)].

B. Cohesive energy

We now calculate the cohesive energy per atom $E_b(\delta_t, \delta_l)$ as a function of the phonon amplitudes δ_t and δ_l . Note that the cohesive energy depends on the density ξ of the electron-hole plasma. For convenience, we consider here the cohesive energy E_b per atom in contrast to our previous work,^{1,3} where we have used the cohesive energy per tetrahedral bond. This causes differences by a factor of 2 because there are two tetrahedral bonds per atom.

We use Harrison's tight-binding theory¹⁸ for the cohesive energy per atom, which has previously been discussed in more detail.^{1,3} It has two contributions,

$$E_b = E_c + E_r, \quad (1)$$

where $E_c < 0$ is an attractive energy due to covalent bond formation and $E_r > 0$ is a repulsive energy. The attractive energy E_c is determined by the electronic density of states $\rho(\epsilon)$ of the conduction and valence bands and the occupation numbers $f(\epsilon)$. Time-resolved measurements of luminescence spectra of laser-excited GaAs (Refs. 19 and 20) showed that a dense electron-hole plasma thermalizes mainly due to electron-electron scattering. The relaxation time decreases strongly for increasing excitation densities. For an excitation density of $4 \times 10^{14} \text{ cm}^{-3}$ the relaxation time²⁰ was about 15 psec and for a density of $7 \times 10^{17} \text{ cm}^{-3}$ a relaxation time of less than 100 fsec had been observed.¹⁹ Here we consider even higher excitation densities of the order of $2 \times 10^{22} \text{ cm}^{-3}$, which is achieved if 10% of the valence electrons are excited into the conduction band. This very dense electron-hole plasma thermalizes very rapidly on a time scale of less than 10 fsec, which is much faster than the movement of the atoms (time scale of 100 fsec). Note that this is in good agreement with previous experiments.²¹⁻²⁴ Thus the electron gas always has a well-defined temperature T_e and we can use the Fermi-Dirac distribution $f(\epsilon, T_e) = \{1 + \exp[(\epsilon - \mu)/k_b T_e]\}^{-1}$ for the electronic occupation numbers. Then the attractive energy is

$$E_c = \int \epsilon f(\epsilon, T_e) \rho(\epsilon) d\epsilon, \quad (2)$$

where the chemical potential $\mu(T_e)$ results from the equation $\int f(\epsilon, T_e) \rho(\epsilon) d\epsilon = 4$ because there are four valence electrons per atom. Time-resolved Raman scattering measurements²⁵ done after pump-laser excitation of GaAs have shown that heat exchange between the electrons and the lattice is relatively slow and occurs on a time scale of several picoseconds. Thus we can neglect heat exchange during the lattice instability. Then the entropy S_e of the electron-hole plasma remains constant ($\delta Q = T dS_e = 0$) and is the important control parameter related to the instability of the lattice. This uniquely determines the temperature T_e of the electron gas through the nonlinear equation

$$\begin{aligned} S_e(T_e) = & -k_b \int_{-\infty}^{+\infty} d\epsilon \rho(\epsilon) \{f(\epsilon, T_e) \ln f(\epsilon, T_e) \\ & + [1 - f(\epsilon, T_e)] \\ & \times \ln[1 - f(\epsilon, T_e)]\} \\ = & \text{const.} \end{aligned} \quad (3)$$

The electronic density of states $\rho(\epsilon)$ of the valence and the conduction bands is determined by a tight-binding Hamiltonian,^{1,18} which depends on the position $\mathbf{R}(\delta_t, \delta_l) = \mathbf{R}_0 \pm \delta_t \mathbf{e}_t \pm \delta_l \mathbf{e}_l$ of the atoms and thus on the phonon amplitudes δ_t and δ_l . As in our previous work³ we use periodic boundary conditions and a cubic supercell containing 64 atoms to diagonalize the Hamiltonian. The electronic density of states $\rho(\epsilon)$ is represented by one special k point,²⁶ which corresponds to using eight inequivalent points in the first Brillouin zone of the usual fcc-lattice representation of the diamond lattice. Similarly as E_c , we obtain the fraction ξ of electrons, which have been excited from the valence band into the conduction band, from

$$\xi = \frac{1}{4} \int_{\text{VB}} \rho(\epsilon) [1 - f(\epsilon, T_e)] d\epsilon, \quad (4)$$

where the integral runs only over the valence band (VB) and counts the number of holes.

The repulsive energy E_r in Eq. (1) arises because of the density-dependent kinetic energy E_{kin} of the electrons.^{18,27} For a free-electron gas the kinetic energy increases for an increasing density n as $E_{\text{kin}} \propto n^{5/3}$ because of the Pauli exclusion principle. From this we conclude qualitatively that the most important contribution to the repulsive energy $E_r \cong \int \delta E_{\text{kin}}[n(\mathbf{r})] d^3r \propto \int [n(\mathbf{r})]^{5/3} d^3r$ comes from the region near the atoms, where the electron density $n(\mathbf{r})$ is highest. Thus E_r is approximately independent of the number of electron-hole excitations, which have only an important effect on the electron density in the bonding regions far away from the atoms. Further, we note that the total electron density of an sp^3 hybridized atom is spherically symmetric and that E_r thus does not depend on bond angles.²⁷ For this reason we use the simple parameterized form

$$E_r(d) = A_1 \exp[-A_2(d - d_0)], \quad (5)$$

which depends only on the bond length d . The parameters A_1 and A_2 have to be determined to give the correct equilibrium bond length d_0 and bulk modulus B at $T_e = 0$. Note that this theory is equivalent to the Born-Oppenheimer approximation in the absence of laser excitations ($T_e = S_e = \xi = 0$).

We now use a phenomenological force-field model of the bonding properties of semiconductors^{1,18} to analyze the numerical results of Eqs. (1)–(5) for the cohesive energy. The total energy consists of two parts. The first part determines the bond lengths. The second part depends on bond angles and makes the diamond structure stable against transitions to more compact metallic structures, such as the β -tin structure. Based on this model we obtain the cohesive energy per atom in terms of powers of the phonon amplitudes δ_t and δ_l . The geometry of the

tetrahedral bonds in the diamond structure and the transverse acoustic- and longitudinal optical-phonon distortions as presented in Sec. II A result in

$$E_b(\delta_t, \delta_l) \cong \frac{\omega_{t,0}^2 M}{2} [1 - a(S_e)] \delta_t^2 + \frac{\omega_{l,0}^2 M}{2} \delta_l^2 + c_1 \delta_t^4 + c_2 \delta_l^4 - \frac{b(S_e)}{2} \delta_t^2 \delta_l^2, \quad (6)$$

where M is the mass of an atom. Without an electron-hole plasma (density $\xi=0$ and entropy $S_e=0$) we have $a(0)=b(0)=0$. The diamond lattice is then a stable minimum of the cohesive energy [Eq. (6)] and $\omega_{t,0}$ and $\omega_{l,0}$ are the frequencies of the transverse acoustic and longitudinal optical phonons. The coefficients $a(S_e)$ and $b(S_e)$ increase with an increasing plasma density ξ and entropy $S_e(\xi)$. Thus the frequency of the transverse acoustic phonon decreases as $\omega_t(S_e) \cong [1 - a(S_e)]^{1/2} \omega_{t,0}$ until the phonon becomes soft for $a(S_e)=1$. For larger densities of the electron hole plasma the transverse acoustic phonon becomes unstable, $[\omega_t(S_e)]^2 < 0$, and the fourth-order term $c_1 \delta_t^4$ defines a new equilibrium position ($c_1 \cong \text{const} > 0$ and $c_2 \cong \text{const} > 0$). The anharmonic interaction term $-b(S_e) \delta_t^2 \delta_l^2 / 2$ then leads to additional longitudinal optical distortions. Thus the equilibrium value for the amplitude of the longitudinal optical phonon shifts towards positive values $\delta_l > 0$, which evens out the distances between the atomic planes (see Fig. 1). Note that the frequency of the longitudinal optical phonon remains nearly unaffected, $\omega_l(S_e) \cong \omega_{l,0}$.

The instability of the diamond structure in the presence of a dense electron-hole plasma has a simple physical interpretation,¹ which follows from Eq. (6) in the context of Eqs. (1)–(5) of our electronic theory for the cohesive energy. Note that in the absence of an electron-hole plasma ($\xi=T_e=0$) there is a strong attractive covalent bonding force due to E_c [see Eq. (2), $\delta E_c \gg 0$ upon an increase $\delta d > 0$ of the bond lengths]. This force is then compensated in the total binding energy E_b [Eq. (1)] by the repulsive force due to E_r [see Eq. (5), the parameters A_1 and A_2 are adjusted to give $\delta E_r = -\delta E_c \ll 0$ and thus $\delta E_b \cong 0$ for $d=d_0$ and $\xi=T_e=0$]. Obviously, this is required for the equilibrium of the diamond structure. However, the attractive covalent bonding forces are strongly affected by a laser-induced electron-hole plasma, because a significant fraction ξ of the electrons is promoted from bonding (VB) states into antibonding conduction-band (CB) states. In a simple bond-orbital picture these attractive forces vanish if bonding and antibonding orbitals are equally occupied [corresponding to $f(\epsilon) \cong 0.5$ and thus $\xi=0.5$] because the respective attractive (bonding, $\delta \epsilon_{\text{VB}} > 0$) and repulsive (antibonding, $\delta \epsilon_{\text{CB}} < 0$) parts of the integrand in Eq. (2) then cancel, such that now $\delta E_c \cong 0$. On the other hand, the electron-hole plasma has only a small influence on the repulsive energy E_r [see Eq. (5)]. Thus a net repulsive force¹ arises between the atoms after the excitation of the electron-hole plasma [see Eq. (1) for the total cohesive energy] because of the decrease in the attractive bonding forces δE_c (from the arguments above it follows that

roughly $\delta E_b \cong 2\xi \delta E_r$). The increase in the bond lengths for large phonon amplitudes δ_t and δ_l (see Fig. 1) then leads to the negative energy terms $[-\omega_{t,0}^2 M a(S_e) \delta_t^2 / 2]$ and $[-b(S_e) \delta_t^2 \delta_l^2 / 2]$ in Eq. (6). The diamond (zincblende) lattice finally becomes unstable against transverse acoustic displacements δ_t for sufficiently dense electron hole plasmas as approximately $a(S_e) \propto \xi$.

It should be noted that the phenomenological bond-charge model^{11,12} does not include the repulsive forces of a laser-induced electron-hole plasma. In this model a weakening of the transverse acoustic phonons only results from a less important decrease of the effective force constant against bond angle distortions. Thus theories^{13–15} based on the bond-charge model would strongly underestimate the ultrafast laser-induced instability of the diamond structure.

The numerical results for the cohesive energy [Eqs. (1)–(5)] will now be used to obtain the dynamics of the lattice distortions.

C. Dynamics of the instability

The frequency of the phonons is obtained from the cohesive energy as

$$\omega_i^2 = M^{-1} (\partial^2 / \partial \delta_i^2) E_b(\delta_t, \delta_l), \quad (7)$$

where $i \equiv (t, l)$ and M is the mass of an atom. Without electron-hole plasma ($\xi \cong 0$) the phonons are stable ($\omega_{i,0}^2 > 0$) and perform harmonic oscillations $\delta_i(t) = \delta_{i,0} \cos(\omega_{i,0} t + \varphi_i)$, where the phase φ_i is free. The amplitudes $\delta_{i,0}$ are estimated from the equipartition theorem as

$$\delta_{i,0}^2 \cong 2k_B T_s M^{-1} \omega_{i,0}^{-2}, \quad (8)$$

where T_s is the temperature of the atomic lattice. In the presence of a very dense electron-hole plasma the transverse acoustic phonon becomes unstable as $\omega_t^2 = M^{-1} (\partial^2 / \partial \delta_t^2) E_b < 0$. Thus the frequency of this phonon becomes imaginary, $\omega_t = i\Omega_t$, where Ω_t is a real quantity. The oscillatory motion then changes into an exponential growth, $\delta_t(t) \propto \exp(-i\omega_t t) = \exp(\Omega_t t)$, as long as the harmonic approximation remains valid. But anharmonic energy terms become important after a short period of time because of the rapidly increasing amplitude $\delta_t(t)$. We thus have to solve numerically the equation of motion

$$M(d^2/dt^2)\delta_i(t) = -(\partial/\partial\delta_i)E_b \quad (9)$$

for both $\delta_t(t)$ and $\delta_l(t)$. The appropriate initial conditions at $t=0$ are $\delta_i(0) = \delta_{i,0} \cos \varphi_i$ and $(d\delta_i/dt)(0) = -\omega_{i,0} \delta_{i,0} \sin \varphi_i$, where $\delta_{i,0}$ is given by Eq. (8) and φ_i is arbitrary. We proceed by fitting a B -spline function to the numerical results for E_b and by calculating the gradient of this function analytically. This makes a fast numerical solution of the equation of motion possible.

III. RESULTS

For our numerical calculation of the cohesive energy $E_b(\delta_t, \delta_l)$ we use Eqs. (1)–(5) and the universal parameters given by Harrison¹⁸ for the tight-binding Hamiltonian of semiconductors. For Si the energy difference between the atomic s and p levels is $\epsilon_p - \epsilon_s = 7.03$ eV. Note that Chadi²⁸ has proposed slightly different parameter values, which yield similar results.³ The equilibrium bond length is $d_0 = 2.35$ Å and the bulk modulus $B = 0.99 \times 10^{12}$ erg cm⁻³, which determines the repulsive interaction E_r . The mass of a Si atom is $M = 28.1$ amu.

As discussed in Sec. II B, all calculations are done for constant entropies S_e of the electron gas, which is the relevant control parameter of the instability. Thus the density ξ of the electron-hole plasma varies slightly and does not remain constant if the structure is distorted. It also should be noted that the number of electron-hole excitations is not well defined if the gap between the conduction and the valence band vanishes. Yet the entropy S_e is difficult to interpret. Thus we present the results in terms of the fraction $\xi_0(S_e)$ of the electrons, which have been excited initially by the laser pulse from the valence band into the conduction band. $\xi_0(S_e)$ is evaluated for the ideal diamond structure [see Eq. (4), $\delta_t = \delta_l = 0$] and corresponds to the initial density of the electron-hole plasma.

In the absence of excitation ($\xi_0 = 0$) we obtain from Eq. (7) phonon frequencies of $\omega_{t,0} = 3.0 \times 10^{13}$ sec⁻¹ and $\omega_{l,0} = 1.2 \times 10^{14}$ sec⁻¹, which are in fair agreement with the experimental values^{29,30} of 2.1×10^{13} and 0.97×10^{14} sec⁻¹. Thus we conclude that our theory gives reasonably accurate quantitative results. For increasing densities ξ_0 we obtained^{1,3} a roughly linear decrease of the square of the frequency of the transverse acoustic phonon ω_t^2 and of the elastic shear constant $c_{11} - c_{12}$. If the density ξ_0 exceeded approximately $\xi_{cr} \cong 8\%$, then both ω_t^2 and $c_{11} - c_{12}$ became negative. A very rapid instability was obtained if significantly more than 8% of the electrons were excited from the valence band into the conduction band ($\xi_0 \gg 0.08$). The present work shows that the longitudinal optical phonon, which has not been considered previously, strongly enhances this instability.

In Figs. 2 and 3 we present the results for the cohesive energy per atom $E_b(\delta_t, \delta_l)$ as a function of the amplitudes of the transverse acoustic and longitudinal optical phonon using Eqs. (1)–(5). The ideal diamond structure ($\delta_t = \delta_l = 0$) serves as a natural reference, thus we put $E_b(0,0) \equiv 0$. As expected, the diamond structure is a stable minimum of the cohesive energy in the absence of the electron-hole plasma (Fig. 2). This changes drastically in the presence of a dense electron-hole plasma. Figure 3 corresponds to the case where 15% of the electrons have been excited from the valence band into the conduction band. Here the diamond structure is an unstable saddle point of the cohesive energy surface. A deep valley has opened, leading down to very large negative energies of $E_b \cong -0.45$ eV. In comparison, our previous calculation,³ which neglected longitudinal optical phonons ($\delta_l \equiv 0$) gave a much shallower minimum for the cohesive

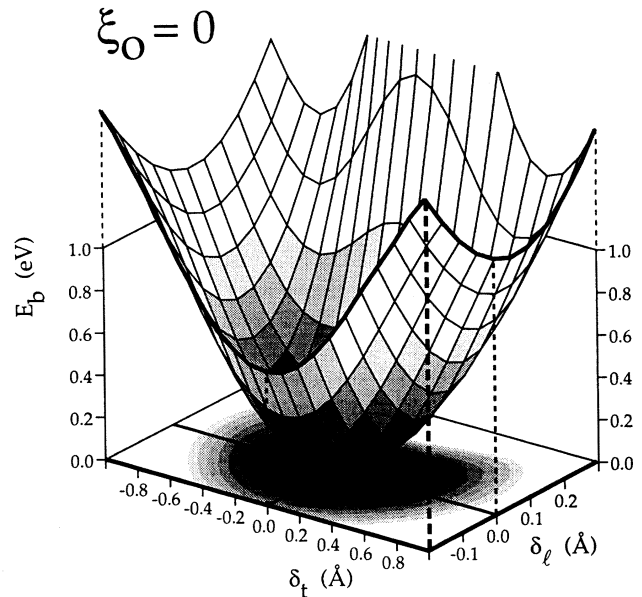


FIG. 2. Cohesive energy per atom E_b of Si [Eqs. (1)–(5)] in the absence of an electron-hole plasma ($\xi_0 = 0$) shown as a function of the transverse acoustic distortion δ_t and the longitudinal optical distortion δ_l of the diamond lattice. Here the ideal diamond structure ($\delta_t = \delta_l = 0$) is a stable minimum of the cohesive energy.

energy of $E_b \cong -0.16$ eV. This agrees qualitatively well with the fact that the transverse acoustic phonon has an effect on only one of the four different tetrahedral bonds [see Fig. 1(a), the length of those bonds increases, which are parallel to the (111) direction], whereas the combination with the longitudinal optical phonon expands all

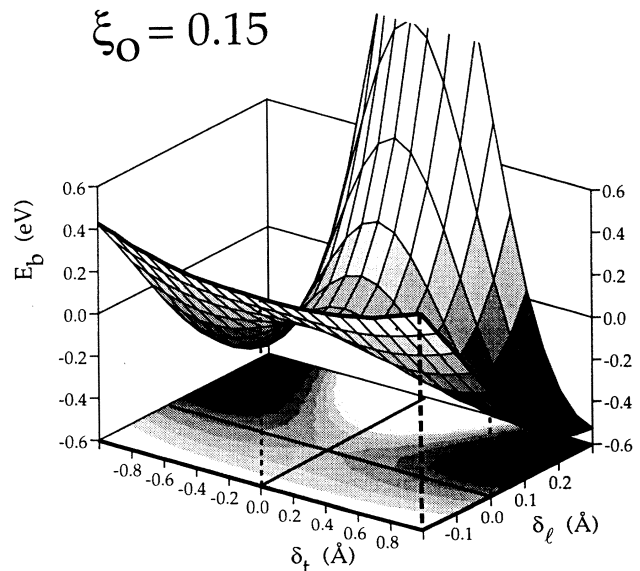


FIG. 3. Cohesive energy for Si [Eqs. (1)–(5)] in the presence of an electron-hole plasma of density $\xi_0 = 0.15$ corresponding to the excitation of 15% of the valence electrons into the conduction band. We use the same representation as in Fig. 2. Note that the ideal diamond structure ($\delta_t = \delta_l = 0$) has become an unstable saddle point.

four bonds. This corresponds to a ratio of 1:4 and is quite close to the ratio for 1:3 obtained from the respective minima of the cohesive energy. Note that the numerical results presented in Figs. 2 and 3 are qualitatively well reproduced by the phenomenological potential function of Eq. (6) and that the instability of the diamond structure at high densities ξ_0 of electron-hole plasma is rather well characterized by the terms $[-\omega_{i,0}^2 M a \delta_i^2 / 2]$ and $[-b \delta_i^2 \delta_l / 2]$ in Eq. (6), which arise from the internal pressure of the electron-hole plasma.¹

In Fig. 4 we show several trajectories resulting from the numerical solution of the equation of motion [Eq. (9)] and using the potential surface $E_b(\delta_i, \delta_l)$ of Fig. 3. The crystal is stable before the laser pulse ($t < 0$) and performs oscillations within the dark shaded region around the ideal diamond structure ($\delta_i = 0$ and $\delta_l = 0$). The corresponding phonon amplitudes are given by the equipartition theorem [Eq. (7)], which results in $\delta_{i,0} = 0.14$ Å and $\delta_{l,0} = 0.04$ Å at room temperature. As discussed in Sec. II C different phases φ_i and φ_l resulted in different initial values of $\delta_i(0)$, $\dot{\delta}_i(0)$, $\delta_l(0)$, and $\dot{\delta}_l(0)$ for the various trajectories. Note that only the first 100 fsec after the excitation of the electron-hole plasma are shown. All trajectories are confined to a narrow region around the bottom of the valley in the potential surface and are very similar to each other. The deviation between the different trajectories is directly related to the initial thermal energy of the lattice. The gap between the valence and the conduction band decreases for increasing distortions δ_i and δ_l , leading to a metallization for a vanishing indirect gap. Qualitatively, we obtain the indirect gap from $\Delta\varepsilon \cong \varepsilon_{CB}(X) - \varepsilon_{VB}(\Gamma)$, where $\varepsilon_{VB}(\Gamma)$ estimates the energy

at the top of the valence band and $\varepsilon_{CB}(X)$ estimates the energy at the bottom of the conduction band. Note that the X point lies near the position of the minimum of the conduction band.³⁰ From an extrapolation for increasing δ_i we then obtain a boundary line in the (δ_i, δ_l) plane, where the indirect gap vanishes, $\Delta\varepsilon(\delta_i, \delta_l) = 0$. This line defines the light shaded region shown in Fig. 4, which has metallic properties. Thus we conclude that the instability results in a transition from the semiconducting diamond structure to a metallic structure with a corresponding change in the plasma frequency and conductivity. This has recently been observed in time-resolved measurements⁷ of the optical reflectivity of laser-excited GaAs. Note that the decrease in the gap between the valence and the conduction band lower the energy of the laser-induced electron-hole plasma. This effectively reduces the energy required for distortions of the diamond (zincblende) lattice, which thus becomes unstable at very high plasma densities.

In Fig. 5 the time dependence of the average displacement $d(t)$ of the atoms from their initial position and the average kinetic energy $E_{kin}(t)$ is shown. These results are derived from the trajectories shown in Fig. 4. Note that within 120 fsec the atomic displacement increases to about 1 Å, which is roughly half the bond length in Si and leads to collisions between the atoms. In the same time, the kinetic energy of the atoms has become larger than 0.4 eV, which corresponds to a temperature far

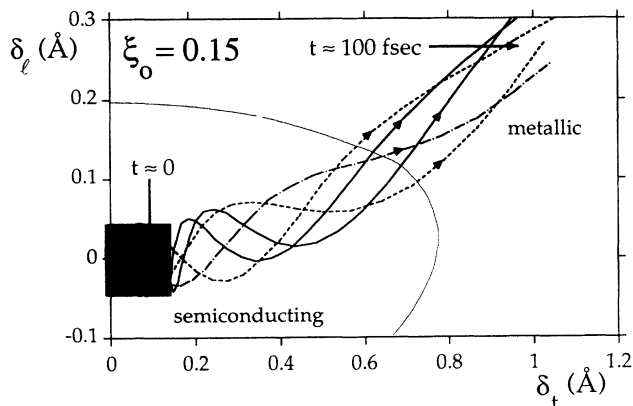


FIG. 4. Time-dependent evolution for the crystal lattice during the first 100 fsec after the excitation of an electron-hole plasma of density $\xi_0 = 0.15$. Note that before the laser pulse ($t < 0$), the crystal is at room temperature and the atomic lattice performs oscillations within the dark shaded area. Five trajectories are shown for $t > 0$ resulting from the equation of motion [Eq. (9)], where the cohesive energy $E_b(\delta_i, \delta_l)$ of Fig. 3 is an effective potential. Inside the light shaded region the gap between the valence and the conduction band vanishes, resulting in metallic properties.

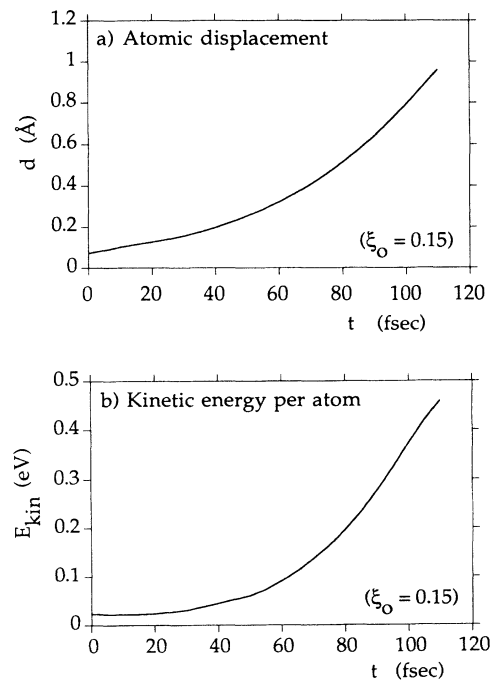


FIG. 5. (a) Time dependence of the average displacement $d(t)$ of the atoms from their position in the ideal diamond lattice. (b) Time dependence of the average kinetic energy $E_{kin}(t)$ of the atoms. The same trajectories are used as in Fig. 4.

above the melting temperature of Si. The atomic collisions redistribute this energy between all phonons of the crystal and a very rapid melting of the crystal occurs. This destroys the diamond structure within a few hundred femtoseconds after the excitation of a sufficiently dense electron-hole plasma, in good agreement with recent experiments.⁶⁻¹⁰

Note that these results also apply to other covalently bonded semiconductors with diamond or zinc-blende structure, such as GaAs. Quantitatively, the different atomic mass M and bond length d result in different phonon frequencies and time scales for the instability. From Harrison's universal tight-binding theory¹⁸ we obtain that the hopping elements $t \propto d^{-2}$. Thus the force constants are $k \propto (\partial^2/\partial d^2)E_b \propto (\partial^2/\partial d^2)t \propto d^{-4}$ and the frequencies scale as $\omega \propto (k/M)^{1/2} \propto d^{-2}M^{-1/2}$. The bond length in GaAs is $d=2.46 \text{ \AA}$ and the average atomic mass is $M=77.8 \text{ amu}$. Thus we obtain that the phonon frequencies in GaAs should be lower by a factor of 1.8 in comparison to Si, which is in good agreement with experiments.³⁰ Then GaAs should have essentially the same lattice instability as Si, but it will require about 200 fsec instead of 120 fsec.

IV. CONCLUSIONS

In summary, we have examined the instability of the diamond lattice of silicon resulting from a laser-induced electron-hole plasma. Detailed results are given for the case, where about 15% of the valence electrons have been excited into the conduction band. We obtain that first the transverse acoustic phonons become unstable. Strong anharmonic interactions subsequently also affect the longitudinal optical phonons. The lattice instability results in an atomic displacement of more than 1 \AA and a kinetic energy of 0.4 eV within about 120 fsec after the laser pulse. The gap between the conduction and the valence band then vanishes and metallic properties are expected. Afterwards the crystal melts very rapidly because of the high kinetic energy of the atoms. These results also apply to GaAs because of dominant tetrahedral covalent bonding. The larger mass of the atoms and the slightly larger bond length result in a slower movement. This increases the time required for the instability to about 200 fsec. Thus we obtain a good quantitative agreement with the observed rapid decrease of the structure sensitive second-harmonic reflection.

*Present address: Albrechtstr. 116, D-12167 Berlin, Germany.

¹P. Stampfli and K. H. Bennemann, Phys. Rev. B **42**, 7163 (1990).

²P. Stampfli and K. H. Bennemann, Prog. Surf. Sci. **35**, 161 (1991).

³P. Stampfli and K. H. Bennemann, Phys. Rev. B **46**, 10 686 (1992).

⁴S. V. Govorkov, I. L. Shumay, W. Rudolph, and T. Schroder, Opt. Lett. **16**, 1013 (1991).

⁵S. V. Govorkov, V. I. Emelyanov, N. I. Koroteev, and I. L. Shumay, J. Lumin. **53**, 153 (1992).

⁶S. V. Govorkov, T. Schroder, I. L. Shumay, and P. Heist, Phys. Rev. B **46**, 6864 (1992).

⁷P. Saeta, J.-K. Wang, Y. Siegal, N. Bloembergen, and E. Mazur, Phys. Rev. Lett. **67**, 1023 (1991).

⁸C. V. Shank, R. Yen, and C. Hirlimann, Phys. Rev. Lett. **51**, 900 (1983).

⁹K. Sokolowski-Tinten, H. Schulz, J. Bialowski, and D. von der Linde, Appl. Phys. A **53**, 227 (1991).

¹⁰H. W. K. Tom, G. D. Aumiller, and C. H. Brito-Cruz, Phys. Rev. Lett. **60**, 1438 (1988).

¹¹R. M. Martin, Phys. Rev. **186**, 871 (1969).

¹²V. Heine and J. A. Van Vechten, Phys. Rev. B **13**, 1622 (1976).

¹³M. Wautelet, Phys. Status Solidi B **138**, 447 (1986).

¹⁴M. Wautelet, P. B. Legrand, and P. M. Petropoulos, Surf. Sci. **163**, 230 (1985).

¹⁵J. Bok, Phys. Lett. **84A**, 448 (1981).

¹⁶L. Kleinman, Phys. Rev. **128**, 2614 (1962).

¹⁷W. A. Harrison, *Electronic Structure and the Properties of Solids* (Freeman, San Francisco, 1980), pp. 198 and 199.

¹⁸W. A. Harrison, *Electronic Structure and the Properties of Solids* (Ref. 17).

¹⁹L. Rota, P. Lugli, T. Elsaesser, and J. Shah, Phys. Rev. B **47**, 4226 (1993).

²⁰D. W. Snoke, W. W. Rühle, Y.-C. Lu, and E. Bauser, Phys. Rev. Lett. **68**, 990 (1992).

²¹D. Hulin, M. Combescot, J. Bok, A. Migus, J. Y. Vinet, and A. Antonetti, Phys. Rev. Lett. **52**, 1998 (1984).

²²W. H. Knox, D. S. Chemla, G. Livescu, J. E. Cunningham, and J. E. Henry, Phys. Rev. Lett. **61**, 1290 (1988).

²³R. W. Schoenlein, W. Z. Lin, J. G. Fujimoto, and G. L. Easley, Phys. Rev. Lett. **58**, 1680 (1987).

²⁴S. D. Brorson, J. G. Fujimoto, and E. P. Ippen, Phys. Rev. Lett. **59**, 1962 (1987).

²⁵J. A. Kash, J. C. Tsang, and J. M. Hvam, Phys. Rev. Lett. **54**, 2151 (1985).

²⁶A. Baldereschi, Phys. Rev. B **7**, 5212 (1973).

²⁷M. Van Schilfgaarde and A. Sher, Phys. Rev. B **36**, 4375 (1987).

²⁸D. J. Chadi, Phys. Rev. B **20**, 785 (1984).

²⁹G. Dolling, *Inelastic Scattering of Neutrons in Solids and Liquids* (International Atomic Energy Agency, Vienna, 1963), Vol. II, p. 37.

³⁰O. Madelung, in *Semiconductors: Group IV Elements and III-V Compounds, Data in Science and Technology*, edited by R. Poerschke (Springer, Berlin, 1991).

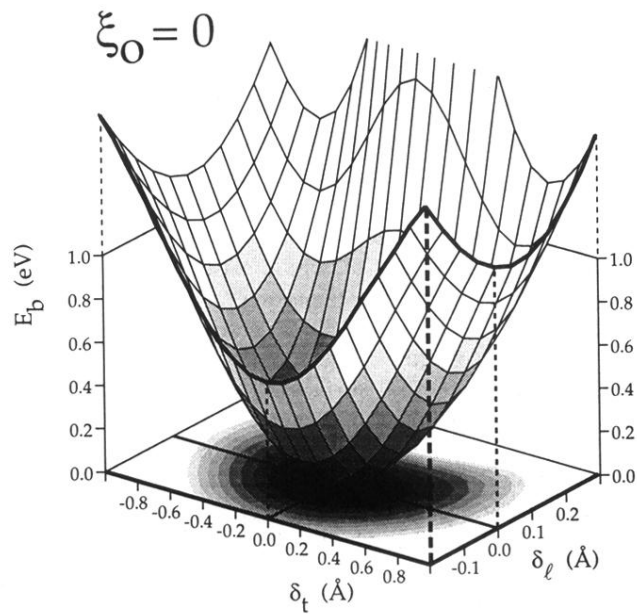


FIG. 2. Cohesive energy per atom E_b of Si [Eqs. (1)–(5)] in the absence of an electron-hole plasma ($\xi_0=0$) shown as a function of the transverse acoustic distortion δ_t and the longitudinal optical distortion δ_l of the diamond lattice. Here the ideal diamond structure ($\delta_t = \delta_l = 0$) is a stable minimum of the cohesive energy.

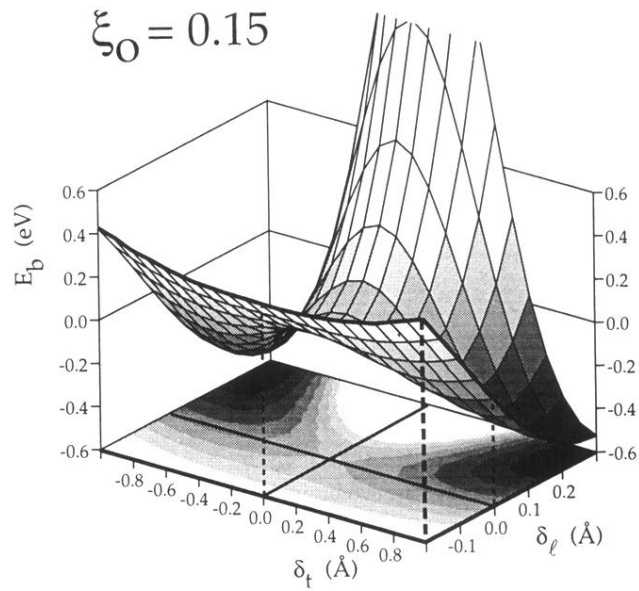


FIG. 3. Cohesive energy for Si [Eqs. (1)–(5)] in the presence of an electron-hole plasma of density $\xi_0=0.15$ corresponding to the excitation of 15% of the valence electrons into the conduction band. We use the same representation as in Fig. 2. Note that the ideal diamond structure ($\delta_t=\delta_l=0$) has become an unstable saddle point.

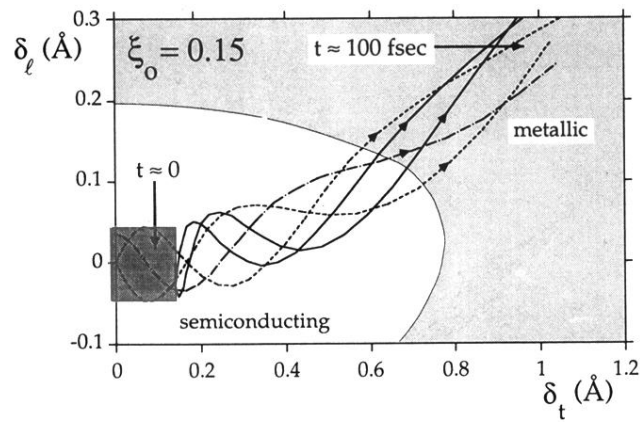


FIG. 4. Time-dependent evolution for the crystal lattice during the first 100 fsec after the excitation of an electron-hole plasma of density $\xi_0=0.15$. Note that before the laser pulse ($t < 0$), the crystal is at room temperature and the atomic lattice performs oscillations within the dark shaded area. Five trajectories are shown for $t > 0$ resulting from the equation of motion [Eq. (9)], where the cohesive energy $E_b(\delta_t, \delta_l)$ of Fig. 3 is an effective potential. Inside the light shaded region the gap between the valence and the conduction band vanishes, resulting in metallic properties.